COMPUTATIONAL MECHANICS 2022
37th conference with international participation
Srní
November 7 - 9, 2022

Supplementary aeroelastic analysis of modified LSA-category aircraft

J. Čečrdle

Czech Aerospace Research Centre (VZLU), Beranových 130, 199 05 Praha Letňany, Czech Republic

Aircraft are required to have a reliability certificate including the aeroelastic (flutter) stability. Flutter analysis must include all applicable configurations of an aircraft in terms of fuel or payload. In the case of the aircraft modification, the appropriate aeroelastic assessment and supplementary analyses are required. Considering the general aviation aircraft, aeroelastic certification is usually based on the ground vibration test (GVT) and on the follow-on analyses using directly the GVT results [1]. The advantage of this approach is its simplicity and cost effectivity. On the other hand, the possibilities for the supplementary analyses in the case of an aircraft modification are limited. Submitted paper presents the practical application of such supplementary analysis.

Subjected aircraft is a two-seat all-composite low-wing LSA-category aircraft. The wingspan is 8.0 m, length is 6.5 m, maximal take-off weight is 600 kg. The design velocity is set as V_D = 300 km/h.

Aeroelastic analysis is based on the experimental data gained by the previously performed GVT of the unmodified aircraft. The changes of the structure and their influence on the structural characteristics are summarised in Table 1.

Table 1. Structure changes and their influence on structural characteristics

Structure change description	Influence on mass and stiffness description
Flap (simple hinge flap instead of a split flap)	No influence on the wing stiffness. Only mass change to be considered.
Aileron (installation of balance weight including the arm)	Control surfaces are considered rigid. No influence on the wing stiffness. Only mass change to be considered.
Wing (reinforced spar web in the central part – inside fuselage)	Influences the wing stiffness. The influence on the appropriate modes to be assessed. Mass change to be considered as well.
Payload increase (pilots, fuel, luggage, parachute)	No influence on the wing and fuselage stiffness. Only mass change to be considered.

The item with the influence on the structural stiffness is the wing spar reinforcement. Therefore, the influences on the appropriate wing and fuselage vibration modes were assessed as summarised in Table 2.

Considering the expected increase in the 1st symmetric wing bending mode frequency, very simple measurement of this mode was performed. Tested aircraft was suspended using a rubber hanger. Sensor instrumentation included two pairs of accelerometers on both sides of the wing and a single accelerometer on the fuselage. The symmetric excitation was realised by a weight release. Measured vibrational time domain response was evaluated. The correct mode was identified within the expected frequency range by the evaluation of the phase

Table 2. Wing spar reinforcement – influence on vibration modes

Mode	GVT freq. (Hz)	Influence description
1st symmetric wing bending	8.57	Symmetric bending deformation of the wing is mainly in the central part of the wing (inside fuselage). Thus, increase in the natural frequency is expected.
1st lateral fuselage bending	10.57	Main bending deformation of the fuselage is at the rear part (behind the cabin). Thus, no significant influence on the fuselage deformation is expected.
1st vertical fuselage bending	11.17	Main bending deformation of the fuselage is at the rear part (behind the cabin). Thus, no significant influence on the fuselage deformation is expected.
1st antisymmetric wing bending	15.03	Antisymmetric bending deformation of the wing is mainly in the out-of fuselage part. Thus, no significant influence is expected.
1st symmetric wing torsion	32.33	Torsional deformation of the wing is mainly in the out-of fuselage part. Thus, no significant influence is expected.

relations among the sensors. The frequency (f), logarithmic decrement (υ) and damping ratio (ζ) were evaluated using standard equations.

As regards to mass changes, the empty weight of the aircraft increased from 280.5 kg to 300 kg (structural changes, parachute) and payload increased from 169.5 kg to 300 kg (pilots, fuel, luggage). The maximal take-of weight increased from 450 kg to 600 kg.

Flutter analyses were performed using g-method. This method transforms aerodynamic matrix into the stiffness matrix (real part) and into the damping matrix (imaginary part). The method generates real physical damping prediction directly at the specified velocities. Analyses were performed at several flight altitudes within the certification envelope (from H = 0 to 3000 m). Velocities were ranging from V = 10 m/s to 200 m/s. Non-matched analysis was employed, i.e., a single (reference) Mach number (M_{REF}) was used within the whole range of velocities. M_{REF} = 0, i.e., incompressible flow was considered. This fact must be considered in the result evaluation. Flutter results up to the certification velocity ($1.2*V_D$ = 100 m/s) may be considered as physically correct as the effect of compressibility is negligible up to this velocity. The results for higher velocities represent just artificial results for evaluation of the rate of reserve with respect to the certification velocity. This is the ordinary practice in aeroelastic analysis. Structural damping was considered using viscous model and common damping ratio (g) of 0.02. This is the realistic estimation of the damping with respect to the results of the GVT. Optionally, g = 0.03, which represents the maximal value acceptable by the regulation standards was used.

Aerodynamic model included the wing, horizontal tail, and vertical tail surfaces. Aerodynamic panels were divided with respect to the geometry including control surfaces and tabs. Interpolation between the structural and aerodynamic model (transfer of displacements

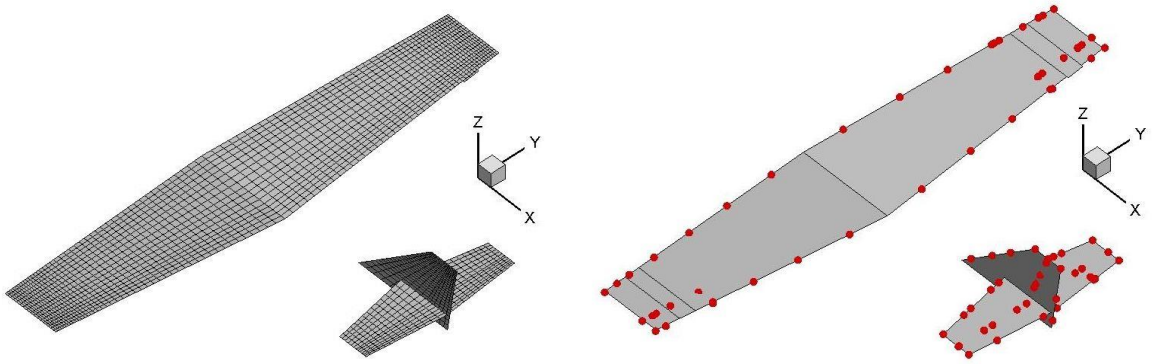

Fig. 1. (a) Aerodynamic mesh, (b) interpolation points

and load between both parts) was realised using Infinite Plate Splines. Appropriate structural points (wing, aileron, aileron tab, etc.) were connected to the appropriate aerodynamic elements. Fig. 1 shows the aerodynamic mesh and the interpolation points.

GVT data (modal model) included 30 modes in total with the frequencies up to 90 Hz. These modes represent vibration modes of the main structural parts (wing, fuselage, vertical tail, horizontal tail) and control surface flapping modes. Full-span model was used, thus both symmetric and antisymmetric modes were included to analysis. Control surface flapping modes were considered for fixed stick (pedals) condition. The reason is that the frequency of the mode with the free stick (pedals) condition is either very close to the frequency of the mode with the fixed stick (pedals) condition (for elevator) or was not measured (otherwise).

Additional mass points representing the structure changes were added into the flutter solution as mass perturbation matrices, which are added into the unperturbed generalized mass matrix. The mass perturbation option provides a change in the mass distribution of the structure without any change within the GVT data.

Analyses included two variants of the fuel load: 26 lt (25 %) and 104 lt (100 %). Identified flutter states are summarised in Table 3 (ordered by the flutter frequency).

Flutter speeds for both analysed configurations are summarised in Fig. 2. It is obvious from the figure that the states of rudder flutter and of aileron flutter are appearing within the certification envelope, i.e., below the velocity of 100 m/s. Considering the structural damping of g = 0.03, which is the maximal value acceptable by regulation standards, the aileron flutter with the character of a hump can be eliminated. Contrary to that, the rudder flutter instability is remaining within the certification envelope even for g = 0.03 (dotted line in the figure).

Due to the above-mentioned fact, the detailed assessment into the rudder flutter instability was performed. First, the flutter primary modes and the main contributing modes were evaluated. Seven modes were evaluated as contributing. From these modes a pair of primary modes (Rudder Flapping, Fuselage Lateral Bending) and a one more significantly contributing mode (Empennage Rolling) were evaluated. Next, the effect of a change in the frequencies of these three modes were evaluated. From this evaluation, the maximal positive effect onto the flutter speed was found for an increase in the Fuselage Lateral Bending mode. However, it is not feasible to make a simple structure change to provide this.

Table 3. Flutter states

Title	Abbr.	~ f_{FL} (Hz)	Description
Rudder flutter	RUDD	9.5	Rudder flapping mode coupling with the empennage rolling mode and with the fuselage lateral bending mode which both induce the fin bending and torsional deformation respectively.
Antisymmetric wing aileron flutter	AILA	11.5	Aileron antisymmetric flapping mode coupling with the wing antisymmetric bending mode, also the lateral engine vibration mode including the wing torsional deformation is contributing.
Wing unsymmetrical flutter	WLA	14.5	This is the wing aileron flutter with the dominant deformation at the port side only. It is caused by the structure unsymmetry.
Symmetric elevator flutter	ELEVS	15.0	Symmetric elevator flapping mode coupling with the fuselage vertical bending and with the tailplane bending deformations. It has a character of a hump instability
Antisymmetric wing aileron flutter	AILA2	16.3	This is another type of the wing bending torsional aileron flutter. It has a character of a hump instability
Wing and elevator flutter	W+E	20.5	Flutter with the dominant deformation at the starboard wing and at the port tailplane. It is caused by the structure unsymmetry.
Antisymmetric elevator flutter	ELEVA	30.6	Antisymmetric elevator flapping mode coupling with the tailplane antisymmetric bending deformations.

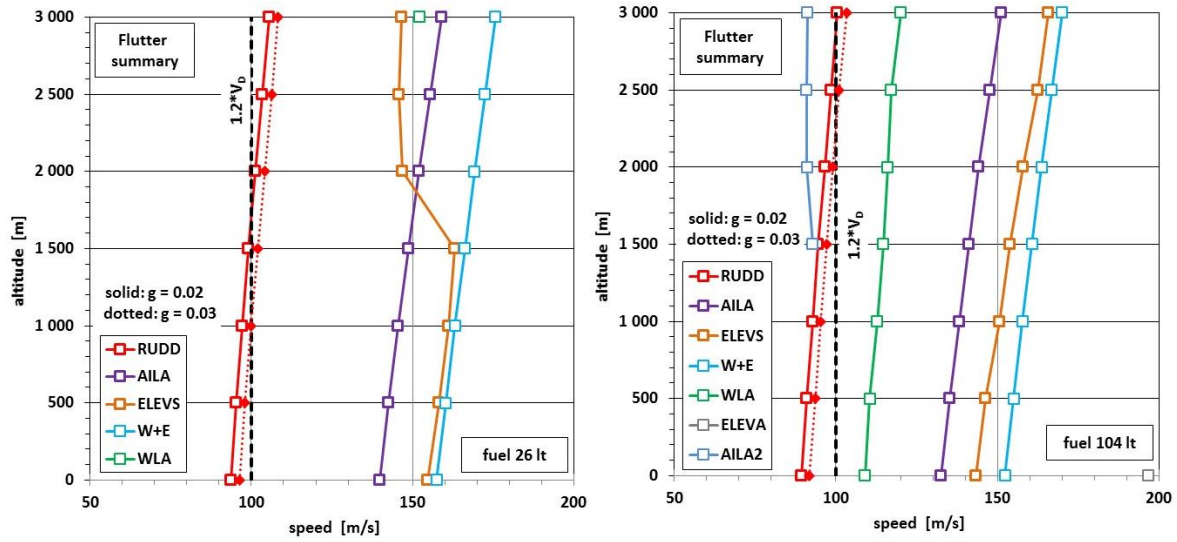

Fig. 2. Flutter speeds (a) fuel 26 lt, (b) fuel 104 lt

Further, the effect of the rudder massbalance was assessed. Note that rudder was not massbalanced. Mass parameters of the rudder structure considering two options of rudder (made of glass-fibre or of carbon-fibre composites) were evaluated. Massbalance weight was simulated at the leading edge of the rudder between both attachment points. Three variants of weight layout (full-length, lower-half, upper-half) were considered. The massbalance weights for a static balance were calculated for these six options. In addition, the conditions of the rudder dynamic balance with respect to the major flutter-contributing modes (Fuselage Lateral Bending and Empennage Rolling) were assessed. In both cases, the static balancing was found to be sufficient also for the dynamic balancing. Next, flutter analyses considering statically balanced rudder were performed for the above-mentioned options. Flutter speeds of the rudder flutter were found sufficiently above the certification velocity. Finally, the optimization of the massbalance weights were performed, i.e., the minimal massbalance weights to keep the flutter speed above the certification threshold were calculated for the above-mentioned options. These calculations were performed for the most critical case, i.e., fuel of 104 lt and H = 0.

To conclude, it may be stated that the requirement of the regulation standard for the design velocity of $V_D = 300$ km/h is fulfilled provided that the appropriate rudder massbalance weight is applied. Otherwise, the reduced value of V_D must be applied for the subjected aircraft.

References

[1] Čečrdle, J., Hlavatý, V., Aeroelastic analysis of light sport aircraft using ground vibration test data proceedings of the institution of mechanical engineers, Part G: Journal of Aerospace Engineering 229 (12) (2015) 2282-2296.